ACS chemical biology

Articles

pubs.acs.org/acschemicalbiology

Chemical Engineering and Structural and Pharmacological Characterization of the α-Scorpion Toxin OD1

Thomas Durek,*[,‡] Irina Vetter,[‡] Ching-I Anderson Wang,[‡] Leonid Motin,[†] Oliver Knapp,[†] David J. Adams,[†] Richard J. Lewis,[‡] and Paul F. Alewood[‡]

[‡]Division of Chemistry and Structural Biology, Institute for Molecular Bioscience, The University of Queensland, St Lucia, Brisbane, Queensland, Australia 4072

[†]Health Innovations Research Institute, RMIT University, Victoria, Australia 3083

Supporting Information

ABSTRACT: Scorpion α-toxins are invaluable pharmacological tools for studying voltage-gated sodium channels, but few structure−function studies have been undertaken due to their challenging synthesis. To address this deficiency, we report a chemical engineering strategy based upon native chemical ligation. The chemical synthesis of α-toxin OD1 was achieved by chemical ligation of three unprotected peptide segments. A high resolution X-ray structure (1.8 Å) of synthetic OD1 showed the typical βαββ α-toxin fold and revealed important conformational differences in the pharmacophore region when compared with other α-toxin structures. Pharmacological analysis of synthetic OD1 revealed potent α-toxin activity (inhibition of fast inactivation) at $Na_v1.7$, as well as $Na_v1.4$ and $Na_v1.6$. In addition, OD1 also produced potent β-toxin activity at $Na_v1.4$ and $Na_v1.6$ (shift of channel activation in the hyperpolarizing direction), indicating that OD1 might interact at more than one site with $Na_v1.4$ and $Na_v1.6$. Investigation of nine OD1 mutants revealed that three residues in the reverse turn contributed significantly to selectivity, with the triple OD1 mutant (D9K, D10P, K11H) being 40-fold more selective for $Na_v1.7$ over $Na_v1.6$, while OD1 K11V was 5-fold more selective for $Na_v1.6$ than $Na_v1.7$. This switch in selectivity highlights the importance of the reverse turn for engineering α-toxins with altered selectivity at Na_v subtypes.

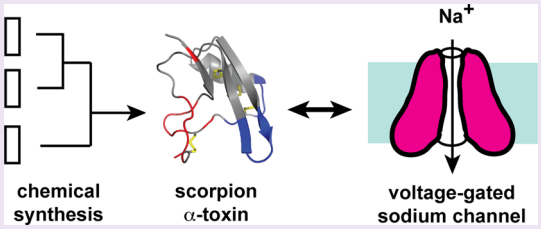

Voltage-gated sodium channels (VGSCs) are essential for initiating and propagating action potentials in most electrically excitable cells of multicellular organisms.[1,2] VGSCs are oligomeric integral membrane proteins and are composed of a pore-forming α subunit, which can associate with one or two auxiliary β subunits. At least nine α-subunit isoforms ($Na_v1.1$−$Na_v1.9$) and four β subunit isoforms (β1−β4) have been identified in vertebrates. The α subunits are composed of four homologous domains (DI−DIV), each containing six transmembrane helices (S1−S6) connected by loops of varying lengths. Although the various α subunit isoforms share at least 50% sequence identity and have remarkably similar functional properties, their tissue-specific expression profile suggests that each isoform has a specialized physiological role in vertebrates.[2] Due to their pivotal role in signal transduction, VGSCs are the targets for many drugs and a large number of biological neurotoxins found in the venom of a wide array of organisms.[3]

Scorpion venoms contain a large number of neurotoxins, which have evolved to attack and immobilize prey and act as a defense mechanism against predators.[4] Due to their high affinity and specificity, individual scorpion toxins have become invaluable pharmacological tools over the past 40 years to help our understanding of VGSC activation and inactivation processes.[3] Long-chain neurotoxins target VGSCs and are polypeptides containing 60−70 amino acids, stabilized by four disulfide bonds. They can be divided into two classes: α-toxins and β-toxins. α-Toxins bind to site 3 of VGSCs, inhibit fast channel inactivation, and have only minor effects on the voltage-dependency of activation while increasing the sodium peak current.[4] In contrast, β-toxins bind to site 4, shift the activation potential to more negative values, and reduce the sodium current amplitude.[3] α-Toxins have a conserved tertiary structure, but their sequence and selectivity toward VGSCs are very diverse.[4] On this basis, α-toxins have been further divided into three subgroups: classical α-toxins, which predominantly act on mammalian VGSCs; insect α-toxins, which bind to insect VGSCs; and α-like toxins that act against mammalian and insect targets. It seems plausible that the different binding surfaces of the toxin and channel are responsible for the different selectivity. However, the molecular basis for this selectivity is poorly understood.[4]

Scorpion toxin OD1 was recently isolated from the venom of the Iranian yellow scorpion (*Odonthobuthus doriae*) and was characterized as an α-like toxin.[5] OD1 is a potent modulator of mammalian $Na_v1.7$ (EC_{50} 4.5 nM) and insect channel para (EC_{50} 80 nM), consistent with α-like toxin pharmacology. However, OD1 only weakly affects mammalian $Na_v1.3$ and $Na_v1.5$ (EC_{50} > 1 μM) and does not affect $Na_v1.2$ and $Na_v1.8$ at

Received: January 6, 2013
Accepted: March 25, 2013
Published: March 25, 2013

all.[5,6] Therefore, it appears to be the first selective high-affinity modulator for mammalian $Na_v1.7$, an important drug target for the treatment of chronic pain.[7] We recently exploited OD1's Na_v selectivity to isolate $Na_v1.7$, selective responses in a novel high-throughput cell-based assay.[8] Unfortunately, a full characterization of most α-toxins is often limited by difficulties in obtaining quantities of pure peptide from the venom or heterologous expression in *E. coli*. In addition, C-terminally amidated forms are difficult to produce in prokaryotic hosts, making it hard to assess the importance of this posttranslational modification for α-toxin function.[9,10] Consequently, we considered chemical synthesis as a viable alternative, as it should overcome the above issues and allow flexible and precise incorporation of unnatural modifications and reporter groups. However, stepwise solid-phase peptide synthesis (SPPS) of long chain α-toxins has achieved limited success, presumably due to the challenging assembly, purification and folding of these relatively large polypeptides.[11]

Here, we report the efficient chemical synthesis of OD1 by combining SPPS, one-pot native chemical ligation, and *in vitro* protein folding. This approach produced α-toxin OD1 on a multimilligram scale, allowing detailed structural and pharmacological characterization. Synthetic OD1 was subsequently crystallized, and its X-ray structure was determined at a resolution of 1.8 Å, confirming its correct covalent structure. Selectivity of the synthetic molecule toward various VGSC isoforms was analyzed using a high-throughput fluorescence assay and patch clamp electrophysiology.[8] Structure–activity studies of nine chemically engineered OD1 mutants identified several reverse-turn analogues with significantly altered selectivity and potency, providing a new starting point for the design of selective sodium channel probes.

RESULTS AND DISCUSSION

Chemical Synthesis. OD1 is a C-terminally amidated polypeptide of 65 amino acids. It contains eight cysteine residues that help stabilize its structure by forming four disulfide bonds.[5] We designed the chemical synthesis of OD1 from three polypeptide segments of about equal length (each ~20 amino acids), as shown in Scheme 1. The three polypeptides were covalently joined by Kent's native chemical ligation (NCL) procedure, a chemoselective reaction between an unprotected peptide equipped with a C-terminal thioester and another unprotected peptide bearing a N-terminal cysteine to form a native amide bond.[12] Recent advances have enabled ligation of three or more polypeptide segments in a sequential one-pot fashion resulting in significantly improved overall yields.[13,14] Individual peptide segments OD1[1–22]-α-thioester, OD1[23–46]-α-thioester, and OD1[47–65] were prepared by manual stepwise Boc solid-phase peptide synthesis (SPPS) in high-yield and purity, as described previously.[15] One-pot native chemical ligation was done in 6 M GdmHCl, 200 mM sodium phosphate, 50 mM mercaptophenylacetic acid, 50 mM triscarboxyethylphosphine hydrochloride (TCEP), pH 6.9 and yielded the fully reduced OD1 polypeptide in good yield (48%, Supporting Information (SI), Figure 1). Folding and formation of the four disulfide bonds was done at RT (22 °C) in 50 mM sodium phosphate buffer (pH 7.5) containing a redox system consisting of 8 mM reduced glutathione and 1 mM oxidized glutathione. The reaction reached equilibrium after 4 h, as evidenced by HPLC analysis (Figure 1), with the principal peak corresponding to natively folded OD1 (isolated yield 40%). The monoisotopic mass of the synthetic material,

Scheme 1. Synthesis of Scorpion Toxin OD1 by One-Pot Native Chemical Ligation of Three Unprotected Peptide Segments[a]

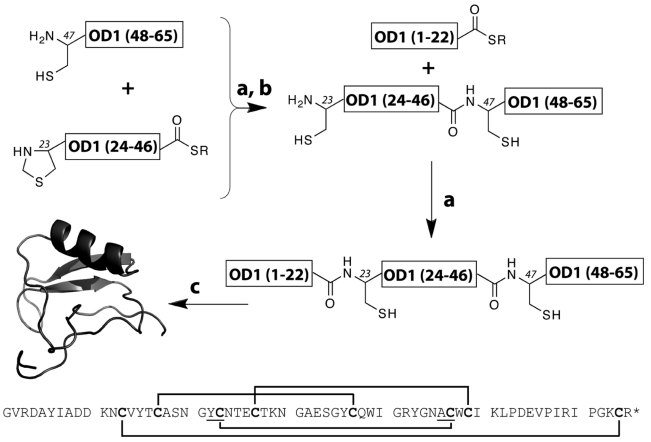

[a]The amino acid sequence is shown in the lower part of the figure with cysteines in bold, ligation sites underlined, and the C-terminal carboxamide indicated by an asterisk. Connectivity of the four disulfides is indicated. (a) Native chemical ligation; (b) Thz → Cys; (c) folding and disulfide formation.

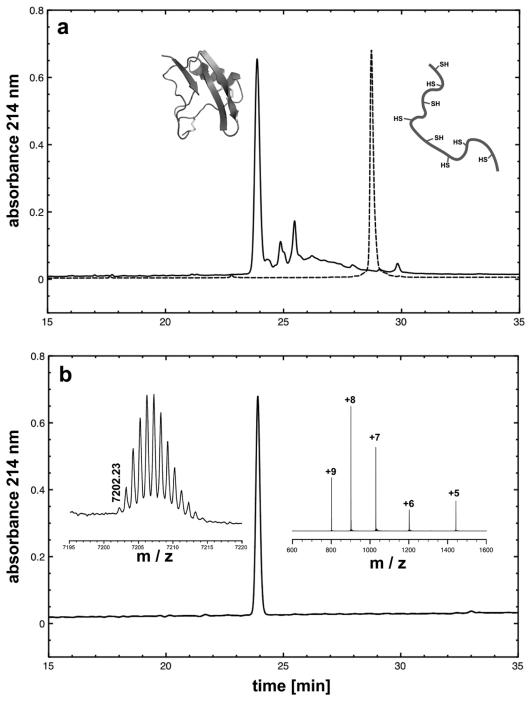

Figure 1. Folding and disulfide formation of synthetic OD1. (a) HPLC analysis of OD1 folding depicting fully reduced OD1 (– –) and the crude folding mixture after 4 h (—). (b) Purified, fully oxidized OD1 (left inset: high-resolution MALDI-MS; right inset: high-resolution ESI-MS).

determined by high-resolution mass spectrometry (7201.49 ± 0.1 (ESI-MS); 7201.23 Da ± 0.1 (MALDI-MS)), is in excellent agreement with the theoretical molecular weight of 7201.22 Da.

Structure of Synthetic OD1. To confirm the authentic covalent structure of the synthetic material and establish a platform for detailed structure–activity relationship studies, we determined the 1.8 Å structure of synthetic wild-type OD1 by X-ray crystallography (SI Table 1). Overall, OD1's structure is

dx.doi.org/10.1021/cb400012k | ACS Chem. Biol. 2013, 8, 1215–1222

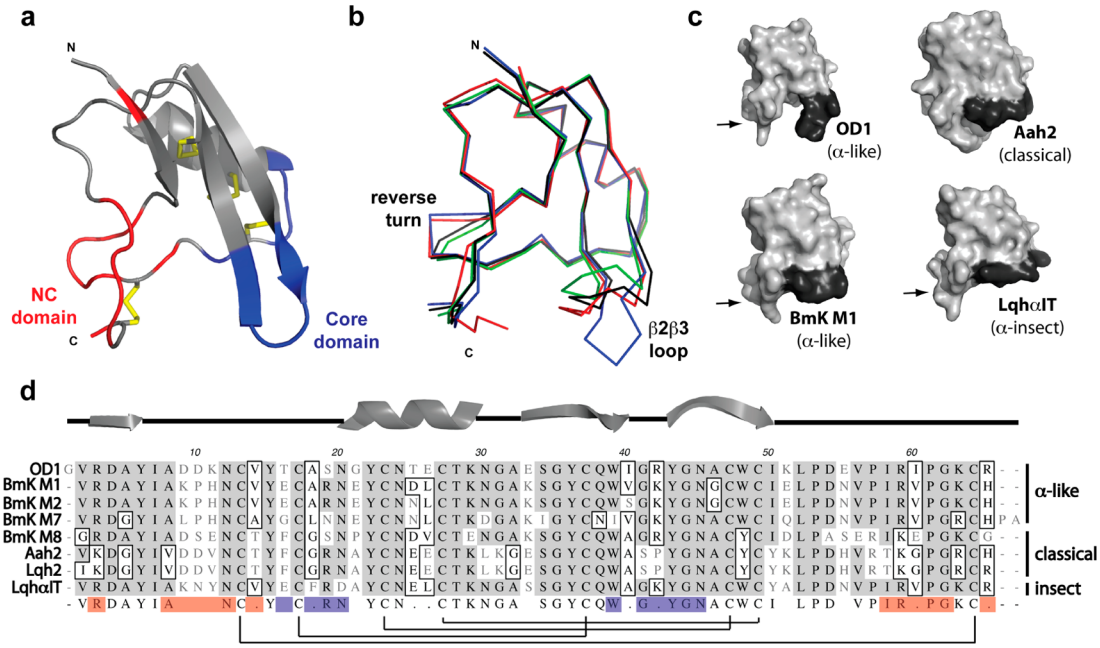

Figure 2. Structure of OD1 (PDB ID: 4HHF). (a) Ribbon representation of OD1. The NC domain and core domain are indicated in red and blue, respectively. Disulfides are shown in yellow. (b) Cα-backbone trace superimposition of OD1 (blue), BmK M2 (yellow, 1CHZ), Aah 2 (red, 1AHO), and LqhαIT (black, 2ASC).[39,40] (c) Surface representation of representative scorpion α-toxins. The $\beta2\beta3$ loop is shaded black. The protruding conformation of the NC domain associated with anti-insect activity is indicated by an arrow. (d) Sequence alignment of OD1 and representative scorpion α-toxin. The NC and core domains are colored red and blue, respectively.

very similar to other known scorpion α-toxin structures (Figure 2a). It is composed of a $\beta\alpha\beta\beta$ core scaffold, from which several loops protrude. Notable structural differences occur in the reverse turn region (residues 8−12), the loop linking the $\beta2$ and $\beta3$ sheets (residues 39−43) and C- and N-termini (Figure 2b). Interestingly, all of these regions have been found to be part of the bioactive surface (pharmacophore) of scorpion α-toxins and are strongly implicated in conferring selectivity and affinity for certain Na_v isoforms.[16,17] Recent studies indicate that α-toxin pharmacophores are divided into two distinct domains: a largely conserved core domain consisting of residues situated in or near the loops connecting the secondary structure elements of the molecular core, and a variable NC domain formed by the reverse turn and residues located in the C-terminal tail (Figure 2a).[18] Extensive mutagenesis and structural studies have led to the hypothesis that conformation of the NC domain plays a critical role in determining α-toxin selectivity, whereas the core domain largely dictates toxin potency.[17] It was suggested that a protruding NC domain conformation is needed for high potency at insect VGSCs (insect-specific and α-like scorpion toxins, e.g., BmK M1, LqhαIT).[16,19] This protruding conformation is characterized by an outward orientation of the side chains of residues 63 and 65 that is supported by a *cis* conformation of the peptide bond between residues 10 and 11.[16,19] Conversely, a flat NC domain conformation found in classical α-toxins, such as Aah 2 and BmK M8, has been correlated with high activity at mammalian $Na_v1.2$.[16] In this flat conformation, which has been correlated to a *trans* peptide bond between residue 10 and 11, the side chains of residues 63 and 65 point inward and form extensive contacts with the $\beta2\beta3$ loop. In the OD1 crystal structure, the peptide bond between residues 10 and 11 is in *trans* conformation and the reverse turn (OD1: ^{8}ADDKN^{12}) aligns structurally well with the same region of Aah 2 (^{7}VDDVN^{11}). However, the side chain of Arg65 forms a hydrogen bond with the carbonyl oxygen of Asp10 and points outward, making the overall NC domain shape resemble that of insect-specific α-toxins (Figure 2c). Thus, OD1's protruding NC domain shape correlates well with its reported high activity on insect channel para (EC_{50} 80 nM) and the lack of activity on mammalian $Na_v1.2$.[5] In contrast, our data indicate that a *trans* conformation of peptide bond 10−11, as observed in the OD1 structure, does not always form a flat NC domain geometry or preclude high affinity for insect VGSCs.

Nevertheless, the most striking structural difference between the OD1 structure and other α-toxin structures occurs in the $\beta2\beta3$ loop, which adopts an extended β-hairpin structure (Figure 2b). In other scorpion α-toxins, the $\beta2$ and $\beta3$ strands are shortened and the $\beta2\beta3$ loop bends away from the core domain toward the NC domain at angles of up to 90° relative to the $\beta2\beta3$ sheet. These conformational differences are accompanied by a different arrangement of hydrogen bonds between the $\beta2$ and $\beta3$ strand peptide backbones and additional interdomain interactions between $\beta2\beta3$ loop residues and the NC domain. The latter interactions are absent in the OD1 structure, as shown in Figure 2b. This is further exemplified by the appearance of a deep, water-filled cleft between the NC and core domains (Figure 2c). As a result, the highly conserved and functionally important hydroxyl group of Tyr6 is exposed, which is not the case in other scorpion toxin structures, where it is buried between the NC and core domains.[20]

Pharmacological Characterization of Synthetic OD1. A systematic functional evaluation of synthetic OD1 was initially done by measuring membrane potential changes on six cloned mammalian VGSCs ($Na_v1.2$−$Na_v1.7$) expressed in human embryonic kidney 293 (HEK293) cells using a fluorescence imaging plate reader (FLIPR).[8,21] This assay allows high-throughput analysis of VGSC modulators, but due to lack of control over the membrane potential it precludes the

dx.doi.org/10.1021/cb400012k | *ACS Chem. Biol.* 2013, 8, 1215−1222

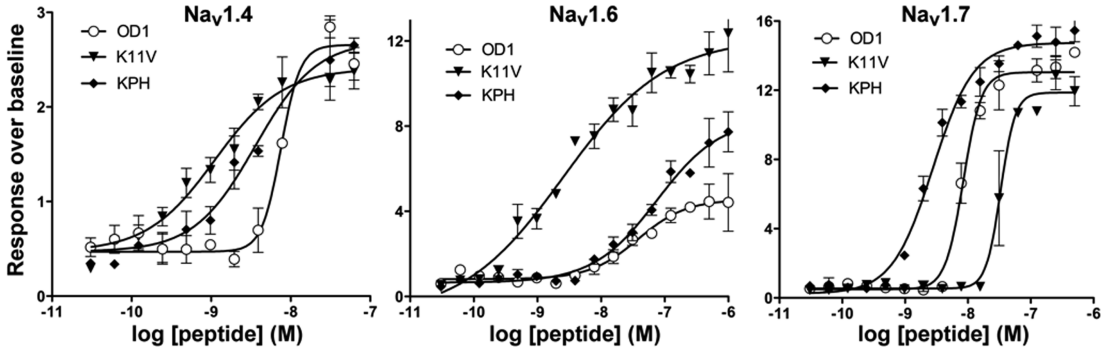

Figure 3. Concentration–response relationships for OD1, OD1$^{D9K,\ D10P,\ K11H}$, and OD1^{K11V} analogues, determined by the FLIPR membrane potential assay.

study of VGSCs at a mechanistic level.[22,23] Fluorescence responses elicited by OD1 in the presence of the alkaloid veratridine were OD1 concentration-dependent and saturable (Figure 3). OD1 potently affected rat Na$_v$1.7 (EC$_{50}$ 7 ± 1 nM), whereas mammalian Na$_v$1.2 (EC$_{50}$ 5.0 ± 2.5 μM), Na$_v$1.3 (EC$_{50}$ 3 ± 1 μM), and Na$_v$1.5 (EC$_{50}$ 4 ± 1 μM) were relatively resistant to activation. These results are consistent with previous studies of OD1 toxin isolated from crude scorpion venom using electrophysiological recordings on *Xenopus laevis* oocytes, confirming the quality of the synthetic material and validity of our high-throughput pharmacological assay.[5,6] OD1 was also found to potently affect Na$_v$1.4 (EC$_{50}$ 10 ± 2 nM) and Na$_v$1.6 (EC$_{50}$ 47 ± 10 nM) for the first time, with Na$_v$1.4 activity observed even in the absence of veratridine. This suggested the toxin may modulate the voltage-dependency of channel activation, an effect normally associated with scorpion β-toxins (SI Figure 3).

To confirm the results of our fluorescence membrane potential assay and examine the effect of the toxin on channel gating, we performed whole-cell patch clamp recording experiments using Chinese hamster ovarian (CHO) cells heterologously expressing human Na$_v$1.4, Na$_v$1.6, or Na$_v$1.7 (Figures 4). OD1 significantly impaired fast inactivation on all channels tested, with EC$_{50}$'s of 9.6 ± 0.1 nM, 30.0 ± 1.0 nM, and 8.0 ± 1.0 nM for hNa$_v$1.4, hNa$_v$1.6, and hNa$_v$1.7, respectively (SI Figure 5). The EC$_{50}$ for hNa$_v$1.7 is in good agreement with the value determined by Maertens et al., who used rNa$_v$1.7 and *Xenopus* oocytes (4.5 ± 0.2 nM),[6] as well as our FLIPR membrane potential assay. The Na^+ peak current amplitude of hNa$_v$1.7 significantly increased at higher OD1 concentrations (100 nM), but those of hNa$_v$1.4 and hNa$_v$1.6 were practically unaffected (SI Figure 6). OD1 induced a long-lasting, sustained current at hNa$_v$1.7. However, this effect was less pronounced at hNa$_v$1.4 and hNa$_v$1.6 (Figure 4a).

OD1's effect on channel activation and steady-state inactivation voltage-dependence was also investigated. The corresponding conductance–voltage curves (Figure 4c) for hNa$_v$1.4 and hNa$_v$1.6 were derived from current–voltage (I–V) relationships in the absence and presence of OD1 (100 nM). While only minor hyperpolarizing shifts (−3 mV) were observed at rNa$_v$1.7 in the presence of OD1 (50 nM),[6] similar concentrations (100 nM) had a profound effect on hNa$_v$1.4 and hNa$_v$1.6 activation. At this concentration, OD1 caused a large hyperpolarizing shift of the half activation voltage by −13 and −19 mV for hNa$_v$1.4 and hNa$_v$1.6, respectively. In contrast, OD1 had little effect on the steady-state inactivation process (Figure 4d). The potential at which sodium conductance was 50% inactivated was unaffected for hNa$_v$1.4 (−59.6 ± 0.2 mV in the control versus −59.4 ± 0.2 mV in the presence of 100 nM OD1) and only slightly shifted to more hyperpolarizing potentials for hNa$_v$1.6 (−72.3 ± 0.2 mV in the control versus −80.1 ± 0.3 mV (n = 3, p > 0.3 in the presence of OD1). Consistent with these small shifts in the voltage-dependence of inactivation, the completeness of hNa$_v$1.4 and hNa$_v$1.6 inactivation was essentially unaffected by the toxin. In contrast, a significant fraction of rNa$_v$1.7 channels remain in the open state, even at membrane potentials where inactivation is normally complete.[6] Taken together, these results demonstrate that the toxin's mechanism of action is significantly different for each of these VGSC isoforms and that our FLIPR membrane potential assay can detect agonistic activity at VGSCs that correlates well with the potencies obtained using conventional electrophysiological approaches.

Molecular Determinants of Toxin Selectivity. To better understand the structural requirements of OD1 selectivity for Na$_v$1.4, Na$_v$1.6, or Na$_v$1.7, we created and analyzed a series of OD1 analogues (Table 1). Mutant proteins were prepared in the same way as wild-type toxin, confirming the robustness of our synthetic approach. Mutating the prominent Tyr6 at the NC and core domain interface reduced potency ∼10-fold without significantly affecting selectivity for Na$_v$1.4, Na$_v$1.6, and Na$_v$1.7. This is consistent with results obtained on the α-like toxin BmK M1[20] and suggests that the tyrosine hydroxyl group is directly involved with the toxin's mechanism of action. Residue 51 was recently implicated in directing toxin selectivity toward mammalian VGSCs.[24] However, the corresponding mutation (OD1^{K51A}) did not significantly affect OD1 activity at Na$_v$1.4, Na$_v$1.6, or Na$_v$1.7. OD1 mutants investigating poorly conserved residues across scorpion α-toxins in the vicinity of the critical NC domain (E55A, E55H, and I60G) did not change potency at Na$_v$1.4 and Na$_v$1.7, although activity on Na$_v$1.6 was reduced. OD1^{E55A} was the most affected, with a 13-fold preference for Na$_v$1.4 and Na$_v$1.7 over Na$_v$1.6, compared with wild-type toxin's 4-fold preference for Na$_v$1.4 and Na$_v$1.7 over Na$_v$1.6.

In a final series of mutants, we investigated the reverse turn (residues 8–12), which appears to be crucial for organizing the overall NC domain conformation.[16,17] Within this region, a central cluster of three amino acids (positions 9–11) varies considerably among scorpion α-toxins. We constructed a triple mutant of OD1, in which these three residues were exchanged by their counterparts in Bmk M1, an α-like toxin active on Na$_v$1.4 and Na$_v$1.5.[25] The potency of the resulting triple mutant for Na$_v$1.4 and Na$_v$1.7 was significantly increased, by 2- to 3-

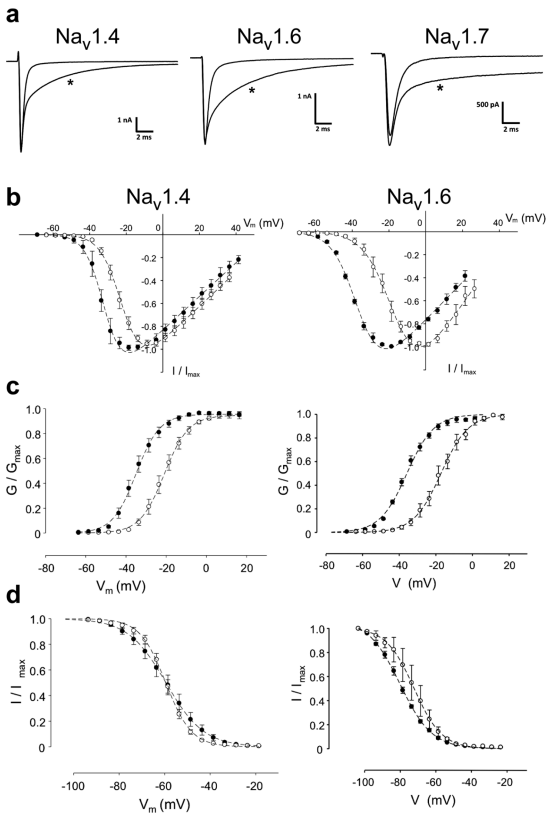

Figure 4. (a) Representative whole-cell Na^+ currents of CHO cells stably expressing human $Na_v1.4$, $Na_v1.6$, and $Na_v1.7$. Currents were elicited by a depolarization step from the holding potential of −100 mV to 0 mV. Asterisks (*) indicate traces recorded in the presence of OD1 (10 nM for $hNa_v1.4$, 30 nM for $hNa_v1.6$, and 10 nM for $hNa_v1.7$). (b) Current−voltage relationships for $hNa_v1.4$ and $hNa_v1.6$ sodium channels in control conditions (open circles) and in the presence of 100 nM OD1 (closed circles). The experimental data were fitted with the Boltzmann equation (dotted lines). Half-peak voltage for $hNa_v1.4$ was −22.0 ± 0.2 mV in the absence and −31.7 ± 0.3 mV in the presence of OD1 (n = 7 each). The corresponding values for $hNa_v1.6$ were −16.5 ± 0.5 mV in the control (n = 5) and −36.4 ± 0.4 mV (n = 3) in the presence of OD1. (c) Effect of OD1 (100 nM) on the voltage dependence of $hNa_v1.4$ and $hNa_v1.6$ activation. OD1 caused a shift in half activation voltage from −21.0 ± 0.2 mV to −34.0 ± 0.3 mV in $hNa_v1.4$, and from −17.2 ± 0.3 mV to −35.8 ± 0.5 mV in $hNa_v1.6$. (d) Effect of OD1 on voltage dependence of $hNa_v1.4$ and $hNa_v1.6$ steady-state inactivation. For $hNa_v1.4$ the potential at which half of sodium conductance is 50% inactivated was −59.6 ± 0.2 mV in the control and −59.4 ± 0.2 mV in the presence of 100 nM OD1. For $hNa_v1.6$, the corresponding values were −72.3 ± 0.2 mV in the control (n = 3) and −80.1 ± 0.3 mV (n = 3, p > 0.3) in the presence of 100 nM OD1.

fold, whereas its activity at $Na_v1.6$ decreased 3-fold, compared with wild-type OD1. As a result, the mutant was >40-fold selective for $Na_v1.7$ over $Na_v1.6$. To mimic the reverse turn of Aah 2, a classical mammalian-specific α-toxin active on $Na_v1.2$ and $Na_v1.4$,[26] we synthesized $OD1^{K11V}$. This mutant exhibited a 5- to 6-fold increase in activity at $Na_v1.6$ and $Na_v1.4$ and a 3-fold reduction in potency at $Na_v1.7$. As a result, there was a 5-fold preference for $Na_v1.6$ over $Na_v1.7$. This suggests residue 11 has a key role in high-affinity scorpion toxin binding to $Na_v1.7$ and $Na_v1.6$, with the former apparently preferring a basic residue (Lys/His) and the latter preferring a neutral residue at this position. The subtype-specific $OD1^{D9K,D10P,K11H}$ and $OD1^{K11V}$ are potentially valuable tools that can be used to

Table 1. Pharmacological Characterization of OD1 and Analogues[a]

OD1 analogues	h1.4	r1.6	r1.7
wt	10 ± 2 (7)	47 ± 10 (8)	7 ± 1 (11)
Y6F	174 ± 73 (3)	384 ± 88 (3)	124 ± 24 (4)
D9K D10P K11H	6 ± 2 (3)	139 ± 47 (3)	3 ± 1 (3)
K11V	2 ± 1 (3)	6 ± 1 (3)	30 ± 4 (3)
K51A	14 ± 4 (3)	49 ± 19 (3)	15 ± 3 (4)
E55A	8 ± 1 (3)	109 ± 8 (3)	8 ± 3 (3)
E55H	7 ± 1 (3)	82 ± 26 (3)	9 ± 1 (4)
I60G	8 ± 1 (3)	73 ± 15 (3)	18 ± 5 (3)
D9K D10P K11H E55A	10 ± 5 (3)	46 ± 24 (3)	0.6 ± 0.4 (3)
K11V E55A	16 ± 10 (3)	3 ± 2 (3)	7 ± 3 (3)

[a]EC_{50} values (in nM) were determined using the FLIPR membrane potential assay, as described in the Supporting Information section. Values are given as mean ± standard error of the mean, and the number of independent experiments is indicated in parentheses.

probe the function and tissue distribution of $Na_v1.7$ and $Na_v1.6$, respectively. Although we could not substantially reduce OD1 activity at $Na_v1.4$, cross-reactivity is less of an issue in neuronal studies, because $Na_v1.4$ expression is (normally) restricted to skeletal muscle fibres and does not colocalize with $Na_v1.6$ or $Na_v1.7$.[27] In anticipation of additive effects, we generated the OD1 double mutant K11V, E55A and a quadruple mutant D9K, D10P, K11H, E55A. The quadruple mutant displayed 10-fold higher potency at $Na_v1.7$, whereas potency was unchanged at $Na_v1.6$ and $Na_v1.4$ when compared to wild-type toxin. In contrast $OD1^{K11V,E55A}$ was equipotent across these isoforms. As a result, neither mutant improved $Na_v1.7/Na_v1.6$ selectivity upon the corresponding single and triple mutants. The absence of cumulative effects strongly suggests that it is the overall architecture of the NC domain, rather than individual residues, that determines toxin selectivity for individual sodium channel subtypes, as was proposed recently.[17] The core domain, on the other hand, largely determines toxin potency irrespective of sodium channel subtype, as exemplified by the $OD1^{Y6F}$ mutant.

According to the conventional view, α- and β-toxins bind to different sites on VGSCs and exert their different activities by stabilizing or destabilizing different conformational states of VGSCs, in particular by interfering with the S4 voltage sensing segments.[28] Specifically, α-toxins bind to site 3 and are believed to prevent outward movement of the S4 segment in DIV to slow fast inactivation, whereas β-toxins bind to site 4 and trap the S4 segment of DII in the activated state.[28−31] These findings correlate well with the observation that the voltage sensors in DI-IV are not functionally equivalent. Those located in DI-III have been linked mostly to channel activation, whereas S4 in DIV is required for channel inactivation.[32] This strict α/β classification of scorpion toxins is now increasingly challenged. Besides OD1, α/β-dual activity has been reported for other scorpion toxins.[33,34] In fact, Bosmans et al. showed that some long-chain scorpion toxins in principle could target any of the four voltage-sensing domains in VGSCs.[35] Our results suggest that OD1 binds selectively to site 3 (DIV) on $Na_v1.7$, and likely binds with high affinity to the same site on $Na_v1.4$ and $Na_v1.6$ to explain its effect on the inactivation kinetics of these channels. However, it is unclear whether the β-toxin effects on these channels is also mediated through site 3 or additional high affinity sites (e.g., site 4). Interestingly, the different Na_v isoforms show markedly distinct susceptibility to some of the tested analogues, particularly to those carrying

dx.doi.org/10.1021/cb400012k | ACS Chem. Biol. 2013, 8, 1215−1222

mutations in the five residue reverse turn ($OD1^{D9K,D10P,K11H}$, $OD1^{K11V}$, and $OD1^{D9K,\ D10P,\ K11H,\ E55A}$), suggesting that α- and β-toxin effects potentially arise through separate sites of interaction, a hypothesis that could be tested by using Na_v chimeras.[35,36]

Conclusions. We have demonstrated that our chemical synthesis approach produces pure α-toxins and analogues on a multimilligram scale, sufficient for detailed structural and pharmacological characterization. Unlike previous studies, which rely on stepwise SPPS to chemically access the relatively long polypeptides,[11] our approach makes use of NCL to "stitch-together" peptide segments of a more manageable size. Because cysteine residues are needed at the site of ligation, NCL is ideal for synthesizing disulfide-rich proteins, such as cytokines and venom-derived molecules. The cysteine residues are highly conserved among scorpion α-toxins, and the intervening sequences are of similar length. Therefore, this strategy has broad applications to other family members.[4] This robust modular approach also allows a diverse range of chemistries, including fluorophores, affinity tags, spin labels, and noncoded amino acids, to be introduced at predetermined locations in large peptides. This makes our approach a powerful tool to generate new ligands to help study ion channels and opens the door to more extensive structure−activity studies. Our pharmacological and structural studies strongly suggest that OD1 (and most likely other scorpion toxins) can differentially interact with closely related VGSC isoforms. Despite sharing a conserved fold, this class of toxins appears to exhibit significant structural variability, especially in their bioactive surface regions: the NC and core domains. As demonstrated, these sites, and the reverse turn in particular, can be engineered to effectively fine-tune toxin selectivity and potency.

METHODS

Peptide Synthesis. Peptides were synthesized by manual *in situ* neutralization Boc solid-phase peptide synthesis (SPPS), as previously described.[15] Peptide α-thioalkylesters corresponding to OD1[1−22]-α-thioester (GVRDAYIADDKNCVYTCASNGY-[COS]Ala) and OD1[23−46]-α-thioester (Thz-NTECTKNGAESGYCQWIGR-YGNA-[COS]Ala) were assembled on HS-CH_2-CH_2-CONH-CH-(CH_3)-COO-CH_2-Pam-polystyrene resin, as described.[37] OD1[47−65] (CWCIKLPDEVPIRIPGKCR-NH_2) was synthesized on 4-methyl-benzhydrylamine (MBHA)-polystyrene resin. OD1[1−22]-α-thioester observed mass 2557.8 ± 0.6 Da, calculated mass (average isotope composition) 2557.8 Da; OD1[23−46]-α-thioester observed mass 2796.9 ± 0.6 Da, calculated mass 2797.0 Da; OD1[47−65] observed mass 2225.6 ± 0.5 Da, calculated mass 2225.7 Da. One-pot native chemical ligation of the three peptide segments as well as folding and formation of the disulfides is described in detail in the Supporting Information section. The OD1 observed monoisotopic mass was 7201.49 ± 0.1 Da (ESI-MS); 7201.23 ± 0.1 Da (MALDI-MS), calculated mass 7201.22 Da.

FLIPR Membrane Potential Assay. HEK293 and CHO cells (all American Tissue Culture Collection, Manassas, VA, USA) were maintained at 37 °C in a 5% humidified CO_2 incubator in Dulbecco's Modified Eagle's Medium (DMEM) containing 10% fetal bovine serum (FBS), 2 mM L-glutamine, pyridoxine, and 110 mg mL^{-1} sodium pyruvate (Invitrogen). HEK293 cells stably transfected with the $rNa_v1.7$ α-subunit were grown in DMEM (Invitrogen), 10% FBS, and 100 μg/mL G418 (Invitrogen). All cells were split every 3−6 days in a ratio of 1:5, using 0.25% trypsin/ethylenediaminetetraacetic acid (Invitrogen). $hNa_v1.2$ and $hNa_v1.5$ were transfected in HEK293 cells using a commercial BacMam transfection system (Invitrogen) following the manufacturer's instructions. Baculovirus solution (2 mL) was diluted with phosphate-buffered saline (3 mL), and 50−70% confluent HEK293 cells were incubated for 2 h at RT, before incubation with enhancer solution in complete medium overnight at 37 °C. BacMam-transfected cells were plated at a density of 10,000 cells/well in DMEM containing 10% FBS and assayed after 24 h. $hNa_v1.3$, $hNa_v1.4$, and hNav1.6 EZCells were purchased from ChanTest Corp (Cleveland, OH, USA), plated on 384-well plates immediately after thawing, and assayed after incubation for a further 24 h at 37 °C in a 5% humidified CO_2 incubator. OD1-induced membrane potential changes in HEK293 and CHO heterologously expressing Na_v isoforms were measured as previously described.[21] Membrane potential dye (red, proprietary composition; Molecular Devices, Sunnyvale, CA) was diluted according to the manufacturer's instructions in physiological salt solution (composition: 140 mM NaCl, 11.5 mM glucose, 5.9 mM KCl, 1.4 mM $MgCl_2$, 1.2 mM NaH_2PO_4, 5 mM $NaHCO_3$, 1.8 mM $CaCl_2$, 10 mM 4-(2-hydroxyethyl)-1-piperazineethanesulfonic acid (HEPES), pH 7.4). Growth media was removed from cells plated on 384-well black-walled imaging plates (Corning) and replaced with 20 μL of red membrane potential dye before incubation of cell plates for 30 min at 37 °C in a 5% humidified CO_2 incubator. Dye-loaded cells were transferred to the $FLIPR^{TETRA}$ imaging plate reader, and fluorescence signals (excitation 510−545 nm; emission 565−625 nm) triggered by OD1 were measured every 2 s for 300 reads. Taking advantage of OD1's ability to potentiate Na_v-mediated responses triggered by the site 2 alkaloid veratridine, veratridine was added, and fluorescence responses were measured for another 300 reads at 2 s intervals. OD1- and veratridine-induced changes in membrane potential, determined in at least 3−5 independent experiments, were analyzed using Screenworks 3.1.1.4 (Molecular Devices). A 4-parameter Hill equation with variable Hill slope was fitted to the data using GraphPad Prism (Version 4.00, San Diego, California). All data, unless otherwise stated, are expressed as the mean ± standard error of the mean.

Electrophysiology. CHO cells stably transfected with human $Na_v1.4$, $Na_v1.6$, and $Na_v1.7$ (Genionics AG) were grown on glass coverslips in F-12 medium (Gibco) supplemented with 9% FBS (Lonza, BW14-502E), 0.9% penicillin/streptomycin (Gibco, 15070-063), and 100 μg/mL hygromycin B (Invitrogen, 10687-010). Na^+ currents were recorded using the whole-cell patch clamp technique with an Axopatch 200B amplifier (Molecular Devices). Under the voltage clamp recording conditions, cells were depolarized to 0 mV from a holding potential of −100 mV every 5 s to elicit VGSC currents. Membrane currents were filtered at 10 kHz, sampled at 100 kHz by a Digidata 1322A interface (Molecular Devices), and recorded using Clampex 10.3 software (Molecular Devices). The patch recording electrodes had resistances of 1.5−2.5 MΩ and were filled with an internal solution containing (in mM): 130 CsF, 10 CsCl, 10 EGTA, 1 $MgCl_2$, 10 HEPES-CsOH, pH 7.2 or 142 KCl, 10 EGTA, 2 $MgCl_2$, 2 Mg-ATP, 10 HEPES-KOH, pH 7.3. The extracellular solution contained (in mM) 140 NaCl, 5.4 KCl, 1 $MgCl_2$, 2 $CaCl_2$, 10 glucose, 10 HEPES-NaOH, pH 7.3. Series resistance was routinely compensated by 90−95%. Capacitive and leakage currents were digitally subtracted using a −P/8 pulse protocol with hyperpolarizing conditioning pulses. All data were analyzed off-line using Clampfit 10 software (Molecular Devices). To determine the effects of OD1 on current inactivation, the ratio of VGSC current at Δt after peak in the presence of OD1 ($I_{\Delta t}^{OD1}$) to the corresponding value in the absence of the toxin ($I_{\Delta t}^{ctrl}$) was used. A similar ratio was used to determine the toxin's effects on peak current amplitude (I_p^{OD1}/I_p^{ctrl}).

Toxin effects were quantified by the ratio of the current measured at a particular time Δt after the peak ($I_{\Delta t}$) to the peak current: $I_{\Delta t}/I_p$. The value of Δt, which is approximately equal to twice the time constant of fast inactivation, was 1.0 ms for $Na_v1.4$ and $Na_v1.6$ and 1.5 ms for $Na_v1.7$. A similar approach to analyzing the toxin's effect on VGSC currents was described previously.[5,6,38] The concentration-dependence for the toxin-induced effect was determined by plotting the parameter $I_{\Delta t}/I_p$ as a function of toxin concentration. Concentration−response relationships were plotted and fitted with a logistic function using SigmaPlot 8 software (Systat, Chicago USA):

$$I_{\Delta t}/I_p = C_0 + (C_1 - C_0)/(1 + (EC_{50}/[OD1])^n)$$

where n is the Hill coefficient, [OD1] is the toxin concentration, and C_0 and C_1 asymptotic values for the ratio of $I_{\Delta t}/I_p$. Results are shown as the mean ± standard error of the mean.

■ ASSOCIATED CONTENT

Supporting Information

Full details for synthesis, structure determination and Supplementary Figures S1−S6. This material is available free of charge via the Internet at http://pubs.acs.org.

Accession Codes

Atomic coordinates and structure factors for OD1 have been deposited in the PDB (ID 4HHF).

■ AUTHOR INFORMATION

Corresponding Author

*E-mail: thomas.durek@gmail.com.

Notes

The authors declare no competing financial interest.

■ ACKNOWLEDGMENTS

This work was supported by a National Health and Medical Research Council (NHMRC) Program grant (569927; P.F.A., R.J.L., D.J.A.); NHMRC Australian Biomedical Postdoctoral (569918, I.V.) and Research (R.J.L.) Fellowships; and The University of Queensland. D.J.A. is an Australian Research Council (ARC) Australian Professorial Fellow. Funding for the FLIPR^{TETRA} was obtained through an ARC LIEF grant (R.J.L., P.F.A.).

■ REFERENCES

(1) Yu, F. H., Yarov-Yarovoy, V., Gutman, G. A., and Catterall, W. A. (2005) Overview of molecular relationships in the voltage-gated ion channel superfamily. *Pharmacol. Rev. 57*, 387−395.

(2) Catterall, W. A. (2012) Voltage-gated sodium channels at 60: structure, function and pathophysiology. *J. Physiol. 590*, 2577−2589.

(3) Catterall, W. A., Cestele, S., Yarov-Yarovoy, V., Yu, F. H., Konoki, K., and Scheuer, T. (2007) Voltage-gated ion channels and gating modifier toxins. *Toxicon 49*, 124−141.

(4) Bosmans, F., and Tytgat, J. (2007) Voltage-gated sodium channel modulation by scorpion α-toxins. *Toxicon 49*, 142−158.

(5) Jalali, A., Bosmans, F., Amininasab, M., Clynen, E., Cuypers, E., Zaremirakabadi, A., Sarbolouki, M. N., Schoofs, L., Vatanpour, H., and Tytgat, J. (2005) OD1, the first toxin isolated from the venom of the scorpion *Odonthobuthus doriae* active on voltage-gated Na+ channels. *FEBS Lett. 579*, 4181−4186.

(6) Maertens, C., Cuypers, E., Amininasab, M., Jalali, A., Vatanpour, H., and Tytgat, J. (2006) Potent modulation of the voltage-gated sodium channel Na(v)1.7 by OD1, a toxin from the scorpion Odonthobuthus doriae. *Mol. Pharmacol. 70*, 405−414.

(7) Cummins, T. R., Sheets, P. L., and Waxman, S. G. (2007) The roles of sodium channels in nociception: Implications for mechanisms of pain. *Pain 131*, 243−257.

(8) Vetter, I., Mozar, C. A., Durek, T., Wingerd, J. S., Alewood, P. F., Christie, M. J., and Lewis, R. J. (2012) Characterisation of Na-v types endogenously expressed in human SH-SY5Y neuroblastoma cells. *Biochem. Pharmacol. 83*, 1562−1571.

(9) Benkhadir, K., Kharrat, R., Cestele, S., Mosbah, A., Rochat, H., El Ayeb, M., and Karoui, H. (2004) Molecular cloning and functional expression of the α-scorpion toxin BotIII: pivotal role of the C-terminal region for its interaction with voltage-dependent sodium channels. *Peptides 25*, 151−161.

(10) Legros, C., Ceard, B., Vacher, H., Marchot, P., Bougis, P. E., and Martin-Eauclaire, M. F. (2005) Expression of the standard scorpion α-toxin AaH II and AaH II mutants leading to the identification of some key bioactive elements. *Biochim. Biophys. Acta 1723*, 91−99.

(11) M'barek, S., Fajloun, Z., Cestele, S., Devaux, C., Mansuelle, P., Mosbah, A., Jouirou, B., Mantegazza, M., Van Rietschoten, J., El Ayeb, M., Rochat, H., Sabatier, J. M., and Sampieri, F. (2004) First chemical synthesis of a Scorpion α-toxin affecting sodium channels: The Aah I toxin *Androctonus australis hector*. *J. Pept. Sci. 10*, 666−677.

(12) Dawson, P. E., Muir, T. W., Clark-Lewis, I., and Kent, S. B. (1994) Synthesis of proteins by native chemical ligation. *Science 266*, 776−779.

(13) Bang, D., and Kent, S. B. (2004) A one-pot total synthesis of crambin. *Angew. Chem., Int. Ed. 43*, 2534−2538.

(14) Durek, T., Zhang, J., He, C., and Kent, S. B. H. (2007) Synthesis of photoactive analogues of a cystine knot trypsin inhibitor protein. *Org. Lett. 9*, 5497−5500.

(15) Schnölzer, M., Alewood, P., Jones, A., Alewood, D., and Kent, S. B. (1992) *In situ* neutralization in Boc-chemistry solid phase peptide synthesis. Rapid, high yield assembly of difficult sequences. *Int. J. Pept. Protein Res. 40*, 180−193.

(16) Karbat, I., Frolow, F., Froy, O., Gilles, N., Cohen, L., Turkov, M., Gordon, D., and Gurevitz, M. (2004) Molecular basis of the high insecticidal potency of scorpion α-toxins. *J. Biol. Chem. 279*, 31679−31686.

(17) Kahn, R., Karbat, I., Ilan, N., Cohen, L., Sokolov, S., Catterall, W. A., Gordon, D., and Gurevitz, M. (2009) Molecular requirements for recognition of brain voltage-gated sodium channels by scorpion α-toxins. *J. Biol. Chem. 284*, 20684−20691.

(18) Gurevitz, M. (2012) Mapping of scorpion toxin receptor sites at voltage-gated sodium channels. *Toxicon 60*, 502−511.

(19) Guan, R. J., Xiang, Y., He, X. L., Wang, C. G., Wang, M., Zhang, Y., Sundberg, E. J., and Wang, D. C. (2004) Structural mechanism governing cis and trans isomeric states and an intramolecular switch for cis/trans isomerization of a non-proline peptide bond observed in crystal structures of scorpion toxins. *J. Mol. Biol. 341*, 1189−1204.

(20) Sun, Y. M., Bosmans, F., Zhu, R. H., Goudet, C., Xiong, Y. M., Tytgat, J., and Wang, D. C. (2003) Importance of the conserved aromatic residues in the scorpion α-like toxin BmK M1 - The hydrophobic surface region revisited. *J. Biol. Chem. 278*, 24125−24131.

(21) Vetter, I., Dekan, Z., Knapp, O., Adams, D. J., Alewood, P. F., and Lewis, R. J. (2012) Isolation, characterization and total regioselective synthesis of the novel muO-conotoxin MfVIA from *Conus magnificus* that targets voltage-gated sodium channels. *Biochem. Pharmacol. 84*, 540−548.

(22) Trivedi, S., Dekermendjian, K., Julien, R., Huang, J., Lund, P. E., Krupp, J., Kronqvist, R., Larsson, O., and Bostwick, R. (2008) Cellular HTS assays for pharmacological characterization of Na(V)1.7 modulators. *Assay Drug Dev. Technol. 6*, 167−179.

(23) Benjamin, E. R., Pruthi, F., Olanrewaju, S., Ilyin, V. I., Crumley, G., Kutlina, E., Valenzano, K. J., and Woodward, R. M. (2006) State-dependent compound inhibition of Na(v)1.2 sodium channels using the FLIPR V-m dye: On-target and off-target effects of diverse pharmacological agents. *J. Biomol. Screening 11*, 29−39.

(24) Zhu, S., Peigneur, S., Gao, B., Lu, X., Cao, C., and Tytgat, J. (2012) Evolutionary diversification of Mesobuthus α-scorpion toxins affecting sodium channels. *Mol. Cell. Proteomics 11*, No. M111.012054.

(25) Wang, C. G., Gilles, N., Hamon, A., Le Gall, F., Stankiewicz, M., Pelhate, M., Xiong, Y. M., Wang, D. C., and Chi, C. W. (2003) Exploration of the functional site of a scorpion α-like toxin by site-directed mutagenesis. *Biochemistry 42*, 4699−4708.

(26) Alami, M., Vacher, H., Bosmans, F., Devaux, C., Rosso, J. P., Bougis, P. E., Tytgat, J., Darbon, H., and Martin-Eauclaire, M. F. (2003) Characterization of Amm VIII from *Androctonus mauretanicus* mauretanicus: a new scorpion toxin that discriminates between neuronal and skeletal sodium channels. *Biochem. J. 375*, 551−560.

(27) Goldin, A. L. (2001) Resurgence of sodium channel research. *Annu. Rev. Physiol. 63*, 871−894.

(28) Cestele, S., and Catterall, W. A. (2000) Molecular mechanisms of neurotoxin action on voltage-gated sodium channels. *Biochimie 82*, 883−892.

(29) Campos, F. V., Chanda, B., Beirao, P. S. L., and Bezanilla, F. (2008) α-scorpion toxin impairs a conformational change that leads to

fast inactivation of muscle sodium channels. *J. Gen. Physiol. 132*, 251−263.
(30) Rogers, J. C., Qu, Y. S., Tanada, T. N., Scheuer, T., and Catterall, W. A. (1996) Molecular determinants of high affinity binding of α-scorpion toxin and sea anemone toxin in the S3-S4 extracellular loop in domain IV of the Na+ channel alpha subunit. *J. Biol. Chem. 271*, 15950−15962.
(31) Cestele, S., Qu, Y. S., Rogers, J. C., Rochat, H., Scheuer, T., and Catterall, W. A. (1998) Voltage sensor-trapping: Enhanced activation of sodium channels by β-scorpion toxin bound to the S3-S4 loop in domain II. *Neuron 21*, 919−931.
(32) Chanda, B., and Bezanilla, F. (2002) Tracking voltage-dependent conformational changes in skeletal muscle sodium channel during activation. *J. Gen. Physiol. 120*, 629−645.
(33) Cologna, C. T., Peigneur, S., Rustiguel, J. K., Nonato, M. C., Tytgat, J., and Arantes, E. C. (2012) Investigation of the relationship between the structure and function of Ts2, a neurotoxin from *Tityus serrulatus* venom. *FEBS J. 279*, 1495−1504.
(34) Loret, E. P., Martineauclaire, M. F., Mansuelle, P., Sampieri, F., Granier, C., and Rochat, H. (1991) An antiinsect toxin purified from the scorpion *Androctonus australis Hector* also acts on the α-sites and β-sites of the mammalian sodium-channel—sequence and circular-dichroism study. *Biochemistry 30*, 633−640.
(35) Bosmans, F., Martin-Eauclaire, M. F., and Swartz, K. J. (2008) Deconstructing voltage sensor function and pharmacology in sodium channels. *Nature 456*, 202−U228.
(36) Knapp, O., Nevin, S. T., Yasuda, T., Lawrence, N., Lewis, R. J., and Adams, D. J. (2012) Biophysical properties of Nav1.8/Nav1.2 chimeras and inhibition by mu O-conotoxin MrVIB. *Br. J. Pharmacol. 166*, 2148−2160.
(37) Hackeng, T. M., Griffin, J. H., and Dawson, P. E. (1999) Protein synthesis by native chemical ligation: Expanded scope by using straightforward methodology. *Proc. Natl. Acad. Sci. U.S.A. 96*, 10068−10073.
(38) Chen, H. J., Lu, S. Q., Leipold, E., Gordon, D., Hansel, A., and Heinemann, S. H. (2002) Differential sensitivity of sodium channels from the central and peripheral nervous system to the scorpion toxins Lqh-2 and Lqh-3. *Eur. J. Neurosci. 16*, 767−770.
(39) He, X. L., Deng, J. P., Wang, M., Zhang, Y., and Wang, D. C. (2000) Structure of a new neurotoxin from the scorpion *Buthus martensii Karsch* at 1.76 angstrom. *Acta Crystallogr., Sect. D: Biol. Crystallogr. 56*, 25−33.
(40) Smith, G. D., Blessing, R. H., Ealick, S. E., FontecillaCamps, J. C., Hauptman, H. A., Housset, D., Langs, D. A., and Miller, R. (1997) *Ab initio* structure determination and refinement of a scorpion protein toxin. *Acta Crystallogr., Sect. D: Biol. Crystallogr. 53*, 551−557.